Low-cycle fatigue behaviour and microstructure of copper and alpha-brass under planar biaxial loading

S. Henkel[1], J. Fischer[1], L. Balogh[2], T. Ungar[2], M. Hermsdorf[1] and H. Biermann[1]

[1] TU Bergakademie Freiberg, Institute for Materials Engineering, Gustav-Zeuner-Strasse 5, 09599 Freiberg, Germany, henkel@ww.tu-freiberg.de
[2] Eötvös University, Department of General Physics, P.O. Box 32, 1518 Budapest, Hungary, ungar@ludens.elte.hu

ABSTRACT. *The low-cycle fatigue behaviour of copper and α-brass CuZn30 was investigated in uniaxial and biaxial tests. Planar biaxial fatigue tests were carried out using cruciform samples with fixed principal stress axes with and without phase shift on a 250 kN servohydraulic tension-compression testing machine in strain control at room temperature. Biaxial stresses were calculated from the elastic unloading of the hysteresis loops. For the biaxial phase shifted loads additional partial unloadings were inserted to get global elastic conditions in the sample. Microcharacterisation was performed by electron microscopy as well as by high-resolution X-ray line profile analysis and microhardness measurements. The biaxial cyclic stress-strain curves and the lifetimes show good agreement with the uniaxial ones using the von Mises equivalent strain hypothesis. The dislocation densities and microhardness values of the biaxial case, however, show significantly lower values compared to the uniaxial case at equivalent von Mises stresses.*

INTRODUCTION

Life estimation for highly and complex loaded engineering components like aircraft components is always a question of assignability. Often, it is impossible to infer the component behaviour from uniaxial tests. Therefore, starting from uniaxial tests a chain of coupon tests, component relating and full scale tests is necessary. The testing of biaxial planar specimens is one chain link. It gives the possibility to study the damage mechanism of low cycle fatigue behaviour of metals in planar stress state on a clearly arranged sample with fixed principal stress axes in the middle of the specimen. Concerning fatigue lifes, Ogata and Takahashi [1] have performed strain controlled tests at elevated temperatures on cruciform samples of an austenitic stainless steel. Some of the phase shifted samples showed extreme low fatigue lives. Doong et al. [2] investigated the microstructure development of stainless steel grades 304 and 310, aluminium and copper under tension-torsion loading with rotating principal stress axes. They found for the non proportional case that planar slip materials exhibit multi slip structures and extra hardening due to the activating of several slip systems.

Table 1. Properties of the investigated materials

Material	R_m [MPa]	$R_{p0.2}$ [MPa]	A_5 [%]	Young´s modulus [GPa]	Grain Size [µm]
Copper	217	78	48	126	90
CuZn30	339	113	65	110	33

MATERIAL AND METHODS

The investigated materials - commercially pure (99.9964%) copper and α-brass CuZn30 (69.2% copper and 30.7% zinc) - are well known model materials for wavy and planar dislocation slip, respectively. Both materials were available as hot-rolled plates with a thickness of 15 mm. The properties from the static tensile test, Young's modulus and grain size are given in table 1.

The tests were performed on a biaxial 250 kN servohydraulic test rig (Instron) using cruciform samples with a thinned central area of diameter 15 mm and 1.6 mm thickness shown in figure 1. The samples were milled and polished mechanically. Total strain controlled load was applied with a frequency of 0.3 Hz using a biaxial orthogonal extensometer. The amplitude in both loading axes was equal while the phase between the loading axes was varied as 0°, 22.5°, 45° and 90°.

Cruciform samples give no direct access to stresses, therefore finite element analysis was widely used to identify them or the “effective area” of the sample. In fact it is an inverse problem for the FEA: The forces and displacements on the grips are known as well as the reacting local strains in the measurement area of the sample. The requested solution is the material law which links both. Up to now the problem is not fully solved especially for material with plastic behaviour. First steps are done in [3] and [4] using cruciform samples and field measurement methods for the strains by image correlation.

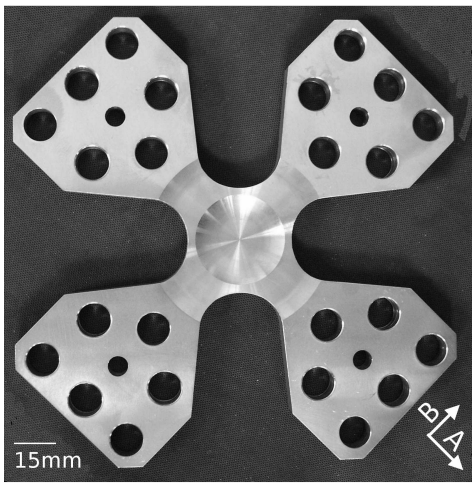

Figure 1. Cruciform sample with load axes directions A and B

In this work the starting of the elastic unloading after changing the ramp direction was used to calculate stresses from local strains by Hooke´s law. It is supposed that the elastic constants are fixed during the test while some researchers found a decrease in the Young´s modulus during LCF tests [5] and of course other influences like damage exist. Figure 2a shows the ramp shape drive signal without phase shift. For cases with phase shift an additional unloading was applied to the drive signal in each cycle to get global elastic unloading conditions in the whole sample (figure 2b). Some subcycles are done as "measurement cycles" with up to 20 small unloadings in both axes to separate the elastic strains to get the stress-strain behaviour during the cycle. Figure 3a shows the drive signal of such a cycle while figure 3b gives the resulting load strain hysteresis loops from the two axes. From the elastic partial unloading the elastic strains and thus the effective stresses in both axes can be calculated.

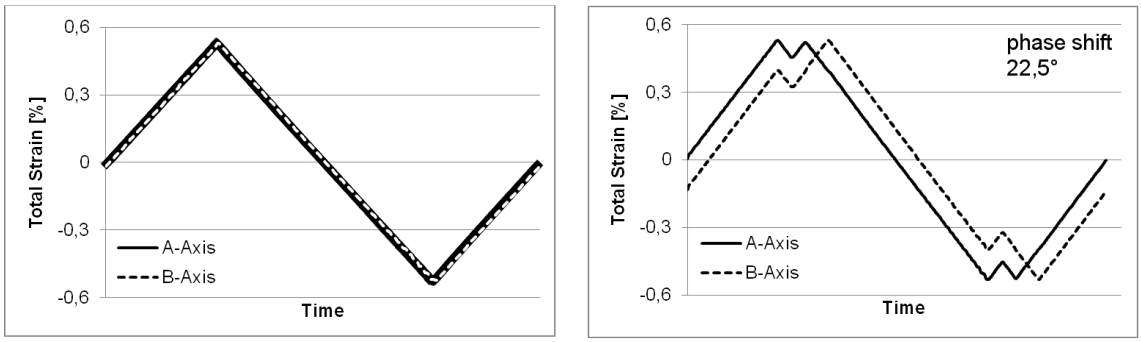

a) b)

Figure 2. Drive signals for strain controlled tests: a) in phase, b) out of phase

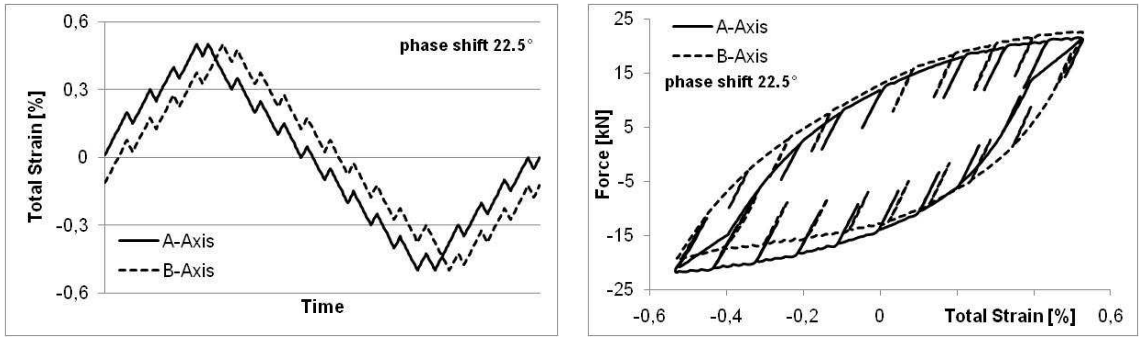

a) b)

Figure 3. Drive signal and load strain hysteresis loop for a stress measurement: a) drive signal with synchronous unloads, b) resulting hysteresis loops with elastic unloads

Uniaxial tests were carried out on a 100 kN servohydraulic testing system using conventional LCF samples at equal von Mises strain amplitudes for comparision. Dislocation densities were measured at Eötvös University, Budapest by X-ray line profile analysis using a high-resolution double-crystal diffractometer [6] on samples deformed to half life ($N_f/2$) for the uniaxial and the biaxial cases with 0° and 22.5° phase shift. For that purpose the inner gage areas of the cruciform samples were

extracted by sinking EDM machining. The samples were then metallographically prepared and electrochemically polished. On one part of the same samples indentation hardness measurements with Vickers indenter and a load from 0 to 500 mN were performed. On selected samples TEM investigations were done on a JEOL JEM 200CX at Eötvös Lórand University Budapest.

RESULTS

The fatigue lives are quite similar in uniaxial and biaxial in phase cases for the same von Mises strain amplitudes, cf. Table 2. The lower life time with increasing phase shift is supposed to result from notch effects of the sample geometry. In these cases the cracks started always from outside the central measurement area. This is supposed to be caused by rotating principal stress axes in these areas under phase shift loads.

Table 2. Life time [cyles] until technical crack

Material	Uniaxial equivalent strain	Strain amplitude in the axes	Uniax.	Biaxial phase shifts			
				0°	22.5°	45°	90°
CuZn30	0.5%	0.28%	18000	13200	13000	8000	10000
	1.0%	0.53%	4000	3500	2000	2000	1500
Copper	0.15%	0.09%		50000	67500		
	0.3%	0.16%	13000	15000	10500		

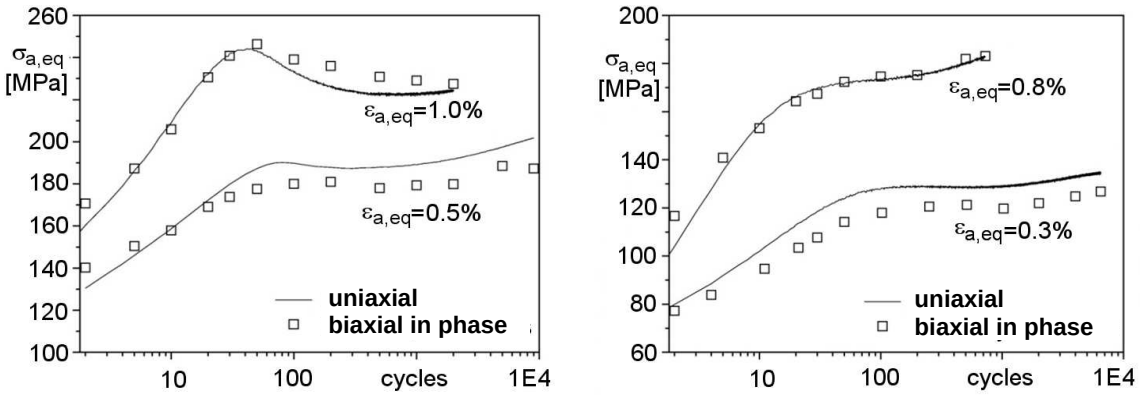

a) b)

Figure 4. Cyclic deformation curves: a) CuZn30, b) copper

Figures 4a and 4b show the cyclic deformation curves of uniaxial and biaxial in phase fatigue tests. In both materials initial cyclic hardening is observed followed by

cyclic softening or cyclic saturation and/or secondary hardening, in accordance with literature [7-9]. Interestingly, the biaxial tests show good agreement with the uniaxial tests. The small differences may be due to uncertainties in the stress determination procedure.

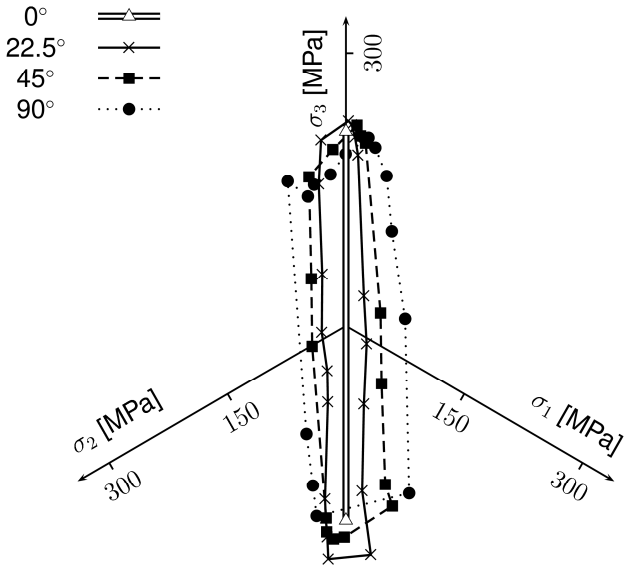

Figure 5. Trace of the octahedral shear stress vector for different phase shifts for CuZn30, 0.53% total strain amplitude in each axis, cycle no. 1000.

For the out of phase case the von Mises hypothesis as a scalar gives smaller stress amplitudes with higher phase shift. For a sine-shape load-controlled test Issler [10] showed that a phase shift of 60° will cause a constant von Mises stress during the whole cycle. So in that case of phase shift the octahedral shear stress interpretion of Nadai [11] gives a vectoral view. Figure 5 shows the octahedral plane with the projected principal stress axes and the trace of the octahedral shear stress vector for one cycle (no. 1000) measured from the partial elastic unloads during this cycle for CuZn30 at 0.53% total

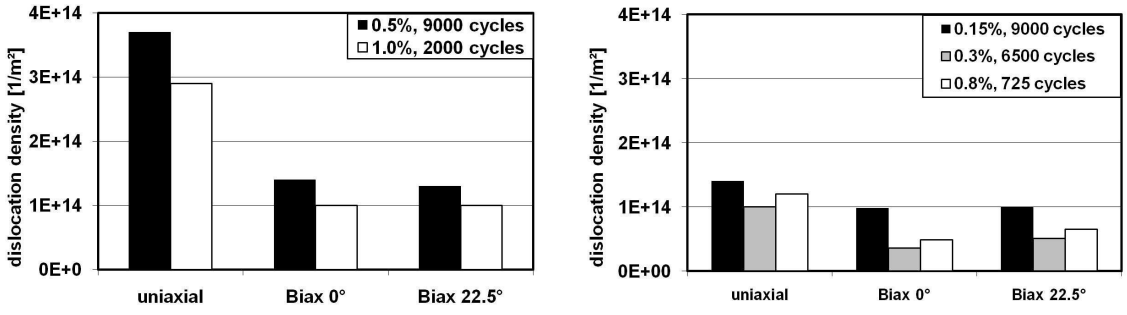

a) b)

Figure 6. Dislocation densities at $N_f/2$: a) CuZn30, b) copper

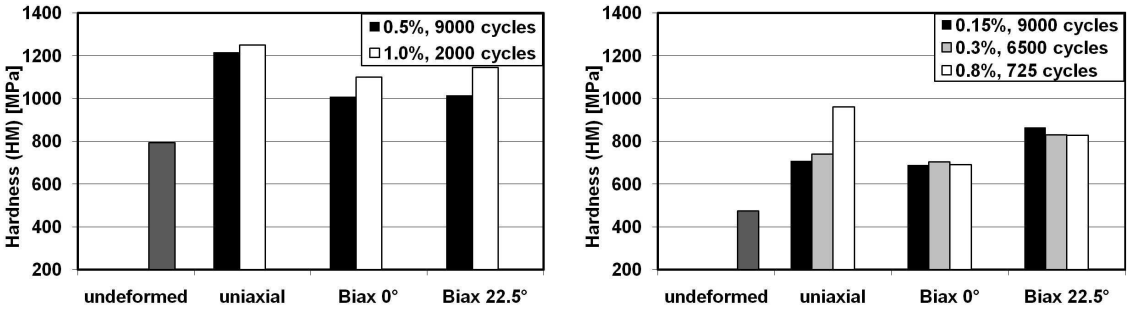

a) b)

Figure 7. Microhardness measurements: a) CuZn30, b) copper

strain amplitude in each axis and a variation of the phase shift (0°, 22.5°, 45° and 90°). It can be seen that the path of the octahedral shear stress vector goes from a straight line at 0° into a box shape with the highest area at 90°. That means that the octahedral shear stress vector is rotating in the octaeder plane while the normal stress direction is fixed.

The dislocation densities are in the biaxial cases significantly lower than in the uniaxial cases (figures 6a and 6b).

In the case of CuZn30 figure 7a shows that the microhardness measurements are in good agreement to the dislocation densities. For copper (figure 7b) the microhardness is slightly lower in the biaxial in phase case than in the uniaxial one. For a phase shift of 22.5° the microhardness is significant higher than in the in phase case and for two amplitudes also higher than in the uniaxial reference tests. This effect is in contrast to the dislocation densities measured on the same samples.

In all cases of copper samples a dislocation cell stucture was observed. Figure 8 shows the microstructures in the TEM for deformed samples at a von Mises equivalent strain amplitude of 0.8%. Similar structures are well-known for uniaxial tests in [12, 13] and for biaxial tension-torsion tests in [2].

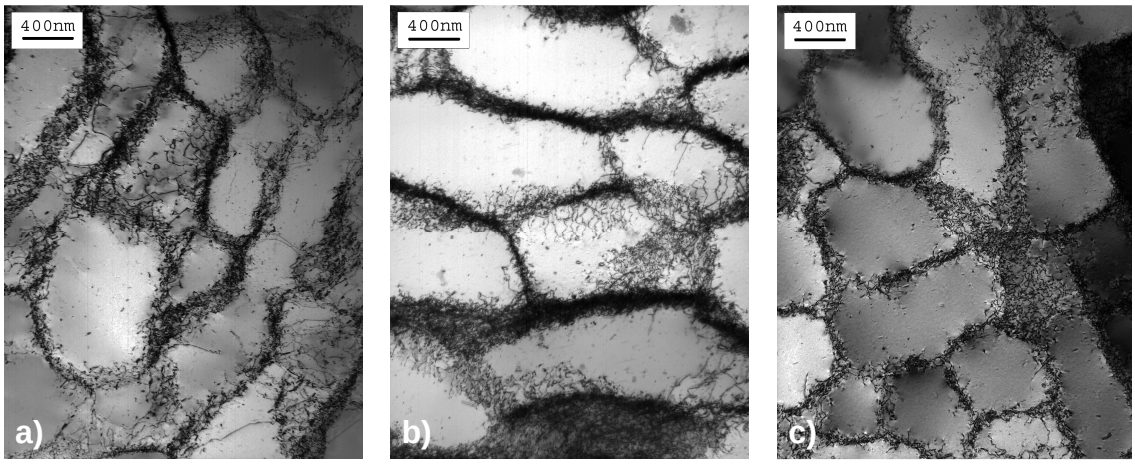

Figure 8. TEM investigations of copper, $\sigma_{a,eq}$ =0.8%; $N_f/2$ = 725 cycles, a) uniaxial, b) biaxial in phase, c) biaxial out of phase (22.5°) fatigue

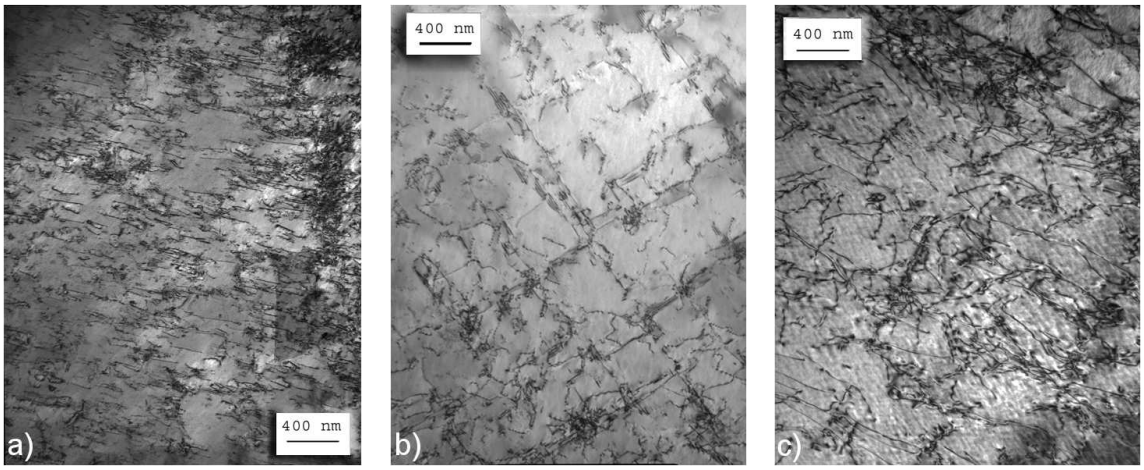

Figure 9. TEM investigations of CuZn15, $\sigma_{a,eq}$ =1%; $N_f/2$ = 2000 cycles, a) uniaxial, b) biaxial in phase, c) biaxial out of phase (22.5°) fatigue

CuZn30 shows planar dislocation structures. However, in the out of phase case they are more irregular, as shown in the TEM images given in figure 9 for the uniaxial, biaxial in phase and biaxial out of phase (22.5°) cases, respectively, at a von Mises equivalent strain amplitude of 1%. A change to a wavy behaviour like reported in [2] for tension-torsion tests on an austenitic stainless steel with rotating principal stress axes was not observed.

SUMMARY AND CONCLUSIONS

The strain and stress amplitudes in uniaxial and biaxial in phase cases using the von Mises equivalent strain hypothesis are in good agreement. Also the fatigue lives are in agreement because life time is mainly controlled by the grains with slip systems of high Schmid factor (high shear stresses). However, dislocation densities are smaller in the biaxial cases. Further investigations have to be done for a full understanding of this behaviour. Out of phase and in phase tests give comparable values of dislocation densities. In addition, life times in the out of phase load cases are affected by sample geometry because of rotating principal stress axes in the notched areas of the samples. In these cases the starting cracks initiate always from outside the measurement area.

ACKNOWLEDGEMENT

Many thanks go to Dr. H.-A. Kuhn, Wieland-Werke AG for providing the test material. Special thank goes to Jáanos L. Lábár from Eötvös University Budapest for the TEM studies.

REFERENCES

1. Ogata, T.; Takahashi, Y. In *Multiaxial fatigue and fracture* E. Macha (Ed.) (1999) Esis publication 25, pp. 101-114
2. Doong, S.-H.; Socie, D. F.; Robertson, I. M. (1990) *Transactions of the ASME* **112** 456-464
3. Lecompte, D.; Smits, A.; Sol, H.; Vantomme, J.; Van Hemelrijck, D. (2007) *Int. J. Solids Struc.* **44**, 1643-56.
4. Périé, J. N.; Leclerc, H.; Roux, S.; Hild, F. (2009) *International J. Solids Struc.* **46**, 2388 - 96.
5. Fournier, B.; Sauzay, M.; Caes, C.; Noblecourt, M.; Mottot, M. (2006) *Materials Science and Engineering: A*, **437**, 183-196
6. Ungar, T. (2004) *Scripta materialia* **51** 777-781
7. Bayerlein, M. (1991) *Wechselverformungsverhalten und Ermüdungsrissbildung von vielkristallinem Kupfer.* Dissertation, Uni. Erlangen-Nürnberg
8. Mughrabi, H. (1978) *Materials Schience and Engineering* **33** 207-223
9. Carstensen, J. (1998) *Structural evolution and mechanisms of fatigue in polycrystalline brass.* Ph.D. thesis Risø-R-1005(EN), Risø National Laboratory, Denmark
10. Issler, L. *Festigkeitsverhalten metallischer Werkstoffe bei mehrachsiger phasen-verschobener Schwingbeanspruchung* (1973) Dissertation, Uni. Stuttgart
11. Nadai, A. (1950) *Theory of flow and fracture of solids.* Volume I
12. Winter, A. T.; Pedersen, O. B.; Rasmussen, K.V. (1981) *Acta Metallurgica* **29** 735-748
13. Zhang, J.; Jiang, Y. (2005) *International Journal of plasticity* **21** 2191-2211